ELSEVIER

Carbohydrate Polymers 45 (2001) 53–59

Carbohydrate Polymers

www.elsevier.com/locate/carbpol

Thermogravimetry/mass spectrometry study of weakly basic starch-based ion exchanger

I. Šimkovic[a,*], E. Jakab[b]

[a]*Institute of Chemistry, Slovak Academy of Sciences, Dubravská cesta 9, 84238 Bratislava, Slovakia*
[b]*Research Laboratory of Materials and Environmental Chemistry, Chemical Research Center, Hungarian Academy of Sciences, Pusztaszeri 59, 1025 Budapest, Hungary*

Accepted 5 May 2000

Abstract

Water-soluble starch was cross-linked with epichlorohydrin in the presence of NH_4OH. The weakly basic ion exchanger prepared this way was made into a salt form with HCl, H_2SO_4, and H_3PO_4. The samples obtained were analyzed with dynamic and isothermal thermogravimetry/mass spectrometry (TG/MS) method in an inert environment. From the dynamic TG/MS plots, it is evident that dehydration is the most important primary reaction observed by this method. The formation of CO_2 as a predominant secondary product has lower intensity by one order of magnitude than water. The third most abundant ion CO (m/z 28) has intensity of the same order as CO_2, while methane, methyl, formyl, formaldehyde and other less important species follow. The calculated rate constants of residue formation as well as gasification from the isothermal experiments fit first-order kinetics, and indicate that the thermal stability of starch is improved by cross-linking with epichlorohydrin. The rate constants of gasification are three orders of magnitude larger than for residue formation, while the activation energies of gasification are smaller than for residue formation. The introduction of amino groups results in a slightly increased rate of thermolysis, while the activation energies are close to unmodified material. Compared to free amine form of the modified starch, the salt form increases the rate of dehydration and decreases the activation energies of gasification especially for H_2SO_4, where SO_2 is formed.

Keywords: Ion-exchanger; Starch; Thermal decomposition; Thermogravimetry/mass spectrometry; Cross-linking

1. Introduction

Cross-linking of starch is often done with epichlorohydrin (E). When this reaction is carried out in the presence of NH_4OH, weakly basic amine groups are incorporated into the material (Šimkovic, Laszlo & Thompson, 1996). By quaternization with 3-chloro-2-hydroxypropyltrimethylammonium chloride (CHMAC), a strongly basic ion exchanger could be prepared (Šimkovic, 1996). The use of choline chloride (CC) instead of CHMAC results in a slightly more ecological product (Šimkovic, 1997). These materials have improved thermal stability (Šimkovic, Antal, Mihálov, Königstein & Micko, 1985a; Šimkovic, Antal, Balog & Plaček, 1985b) and could be used for flame retarding applications (Šimkovic & Csomorová, 1998; Šimkovic, Pastýr, Antal, Balog, Košik & Plaček, 1987b) as well as paper additives (Antal, Ebringerová & Micko, 1991). The weakly basic ion-exchangers prepared from starch by cross-linking with epichlorohydrin in the presence of NH_4OH (SEA) might also find similar applications. That is why they were studied with pyrolysis–gas chromatography/mass spectrometry (Py–GC/MS) to get an insight into the mechanism of their thermal degradation (Šimkovic, Francis & Reeves, 1997). In the present study, we have used TG/MS method to study more about the initial steps of their degradation. This method was applied with success for the study of polysaccharides (Antal, Várhegyi & Jakab, 1998; Šimkovic, Varhegyi, Antal, Ebringerová, Székely & Szabo, 1988), lignins (Jakab, Faix, Till & Székely, 1993; Jakab, Faix, Till & Székely, 1995), and almond shells (Conesa, Marcilla & Caballero, 1997). There is a lack of data on thermolysis of starch using TG or TG/MS methods as seen from reviews on thermolysis of starch (Greenwood, 1967; Tomasik, Wiejak & Palasinski, 1989), where mostly dynamic TG analysis was used (Aggarwal, Dollimore & Kim, 1997). In this work, the rate constants of char as well as gas formation were calculated simultaneously from the isothermal TG experiments for the first time by the linear regression method. Due to a constant temperature, we consider these conditions

* Corresponding author. Tel.: +42-17-5941-0289; fax: +42-17-5941-0222.
E-mail address: simkovic@savba.sk (I. Šimkovic).

0144-8617/01/$ - see front matter
PII: S0144-8617(00)00230-7

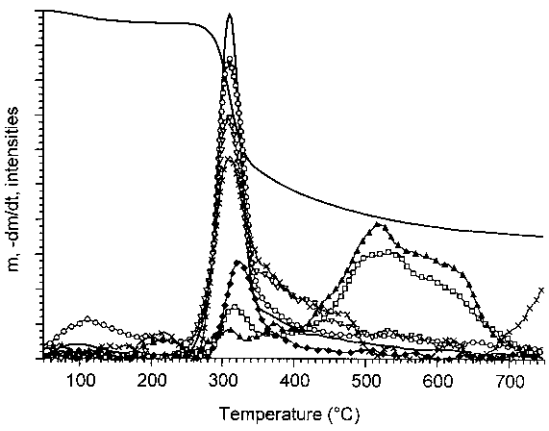

Fig. 1. TG/MS plot of starch: —, TG and DTG curves; -○-, water (*m/z* 18); -▽-, carbon dioxide (*m/z* 44); -×-, carbon monoxide (*m/z* 28); -□-, methyl ion (*m/z* 15); -△-, methane (m/z 16); -◆-, formyl ion (*m/z* 29).

simpler than the use of non-isothermal reaction kinetics (Várhegyi, Antal, Székely & Szabo, 1989). The goal was to find out how inorganic ions in the salts of the starch amines affect the decomposition process.

2. Experimental

Partially hydrolyzed, water-soluble potato starch (S; ZŠ, Dolná Krupá, Slovakia; $M = 19\,060$ Da, determined osmometrically); $[\alpha]^{20} = +154.0°$ (C 1; H_2O) was used without further treatment. SE derivative was prepared by cross-linking S (1.62 g; 0.01 mol) with *E* (7.82 ml; 0.1 mol) in water (9 ml; 0.5 mol) and in the presence of NaOH (4 g; 0.1 mol) applying 24 h stirring at room temperature, dialysis, filtration and subsequent freeze drying (115% yield; N = 0%, C = 44.69% H = 6.87%). Under the same conditions, but in the presence of NH_4OH (14.8 ml of 26% solution) SEA derivative (119% yield; N = 3.05%, C = 42.49% H = 7.38%) was obtained. Part of SEA (0.25 g) was recycled with 5% HCl, H_2SO_4, or H_3PO_4 (100 ml) by stirring for 48 h at room temperature, subsequently washed with excess of deionized water and lyophilized. In this way, SEA–HCl (80% yield; Cl = 4.17%, N = 2.19%, C = 41.79%, H = 6.88%); SEA–H_2SO_4 (59% yield; S = 3.66%, N = 2.27%, C = 39.03%, H = 6.75%); and SEA–H_3PO_4 (43% yield; P = 2.30%, N = 1.98%, C = 40.03%, H = 6.74%) sample were obtained.

The TG/MS experiments were run as described previously (Jakab et al., 1995). The TG/MS system consists of a Perkin–Elmer thermobalance and a Hiden HAL 301/F PIC quadrupole mass spectrometer. Approximately 2–3 mg samples were heated in an argon atmosphere at a 10 K/min heating rate in the dynamic experiments. The mass spectrometer operated at 70 eV electron energy in electron impact ionization mode. The MS intensities were normalized on the sample mass and the intensity of ^{38}Ar isotope of the flushing gas. The following corrections were carried out by the computer for the fragment ions: *m/z* 16 ion of H_2O and CO_2 was subtracted, thus *m/z* 16 represents methane; *m/z* 28 fragment ion of carbon dioxide was subtracted, thus *m/z* 28 ion represents CO; *m/z* 29 and 30 were corrected by the fragment ions of CO. The rate constants were calculated from isothermal TG data by the linear regression method and values of the first 2 min after stabilization at targeted temperature were used, which fitted the regression coefficient value higher than 0.95. The targeted temperatures were reached at 20 K/min rate. The standard deviation of TG and DTG curves is about 2%. The MS curves have higher standard deviation and it varies with the compound detected (polarity, molecular mass, etc.). For polysaccharides, it could be about 10%.

3. Results and discussion

3.1. Products of dynamic experiments

The TG/MS plot of starch is shown in Fig. 1. The water and carbon dioxide ions have maxima at about the same temperature as the DTG curve (Table 1). The formation of water might be initiated by homolytic splitting of hydroxyl groups from the pyranose ring. It is most probable that the formed hydroxy radical withdraws hydrogen from the environment to form water. This must initiate free radical recombination on bonds next to the unpaired electron formed by this process. If the dehydration takes place by heterolytic mechanism, then it must be initiated by some proton or hydroxyl anion, which is less probable due to absence of water at elevated temperatures. The water formed by dehydration might initiate some secondary dehydration by ionic mechanism. The formation of CO_2 and CO might be a result of recombination of free radicals formed on carbon after splitting of C–O bond with the closest available oxygen of pyranose ring. According to Table 1, the fourth most abundant ion is methane, which is related to methyl, the fifth ion in intensity. Because the shape of *m/z* 15 and 16 curves is similar above 400°C, we assume that both ions are indicative of methane. However, *m/z* 15 ion represents also a CH_3^+ fragment ion from other products below 400°C (e.g. methanol, acetone). The sum of their intensities is less than the half of CO_2 value. Because there were no 5-hydroxymethylfuraldehyde ions (*m/z* 126) observed, furaldehyde might be formed from 1,6-anhydro-α-D-glucofuranose by releasing formaldehyde as hypothesized before (Greenwood, 1967). Most of the ions have their maxima close to DTG maximum except for methane with maximal intensity at 520–539°C (Table 1). It is evident that CO_2 and CO are formed subsequently from all oxygen-containing segments as seen from the shoulder of these ion curves starting at 350°C and continuing up to 500°C.

Table 1 compiles the intensity values (peak areas) of individual ions and the temperatures of their maxima for all the samples. It also shows two parameters of the DTG

Table 1
TG/MS data of the measured samples

Value	S	SE	SEA	SEA–HCl	SEA–H_2SO_4	SEA–H_3PO_4
T_{DTG}(°C)	308	341	288	257	265	278
DTG_{max} (%/s)	0.174	0.217	0.167	0.220	0.115	0.255
m/z 15	8510[a]	9550	15800	17000	17100	8170
		374[b]	310			
	539	540[c]	533[c]	531	543	547
m/z 16	10090	7740	18000	21600	23300	12500
	520	517	528	544	547	543
m/z 18	310000	200000	280000	330000	360000	360000
	307	347	289	258	269	280
m/z 27	1400	5100	4200	3600	3350	2200
	324	384	331	477	351	289
m/z 28	24200	26100	32500	15700	14000	14000
	309	356	296	278	244	286
m/z 29	4460	11600	8620	5300	4100	2200
	323	372	315	270	272	286
m/z 30	2500	6000	4750	3300	3400	2400
	324	369	331	344	270	283
m/z 31	570	1590	1750	800	960	500
	316	373	322	225	238	278
m/z 43	1580	4900	4620	2300	1680	1420
	317	371	329	322	372	286
m/z 44	43000	26000	47000	28000	30000	28000
	306	351	291	264	345	284
m/z 58	200	870	670	390	300	210
	319	381	322	364	356	284
m/z 84	140	140	180	100	70	60
	322	343	306	262	260	278
m/z 95	100	80	100	70	60	60
	310	386	315	265	342	282
m/z 96	100	90	130	80	70	70
	313	355	303	268	261	279

[a] Integrated intensity values (peak area) given in arbitrary units.
[b] Temperature (°C) of the intensity maximum of the mass spectrometric ions.
[c] Temperature of the second most intense maximum.

curves such as temperature values of the DTG maximum (T_{DTG}) and the maximal rate of decomposition (DTG_{max}) under dynamic conditions. The yields of char residues are listed in Table 2. Under the conditions used, the char residue at 750°C is higher than obtained on cellulose or xylan in a thermobalance with different geometry at the same heating rate (Šimkovic et al., 1985a; Šimkovic, Durindová, Mihálov, Königstein & Ambrovic, 1986; Šimkovic, Hirsch, Ebringerová & Königstein, 1987a; Šimkovic, Balog & Csomorová, 1995), and the char decreases in the order: SEA–H_3PO_4 > S > SEA–H_2SO_4 > SEA–HCl > SEA > SE. As shown in Table 1, the temperatures of the maximum decomposition rate (T_{DTG}) are decreasing as follows: SE > S > SEA > SEA–H_3PO_4 > SEA–H_2SO_4 > SEA–HCl, while their rate values (DTG_{max}) are in order: SEA–H_3PO_4 > SEA–HCl > SE > S > SEA > SEA–H_2SO_4. The predominant ion observed is water (*m/z* 18), while the second most abundant ion CO_2 (*m/z* 44) has intensity lower by one order of magnitude in the observed temperature range. Although can not be stated categorically from TG/MS, it is evident that water is a primary reaction product, while the majority of other ions are secondary or consecutive or parallel reaction products.

The ion *m/z* 28 represents mostly carbon monoxide and to a lesser extent aliphatic molecules. Aliphatic molecules produce *m/z* 28 and 27 ions in comparable amounts. However, from the starch sample, the abundance of *m/z* 27 is an order of magnitude lower than that of *m/z* 28, indicating that the formation of aliphatic fragments is less

Table 2
Yield of products (%) normalized to the original mass of samples

Sample	Char[a] (%)	Water (%)	Other products[b] (%)	Water/total volatiles[c]
S	35	33	32	0.51
SE	12	21	67	0.24
SEA	18	30	52	0.37
SEA–HCl	26	35	39	0.47
SEA–H_2SO_4	31	38	31	0.55
SEA–H_3PO_4	41	39	20	0.66

[a] TG residue at 750°C.
[b] By difference.
[c] Included water.

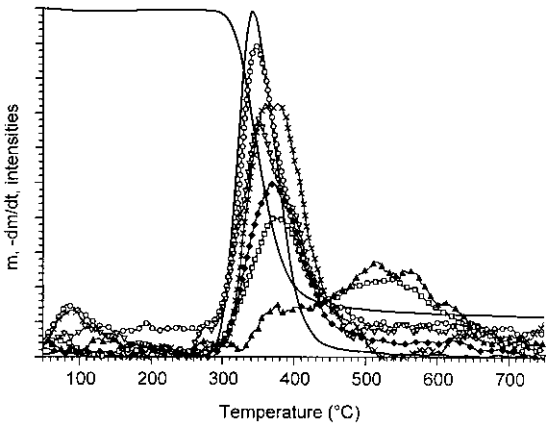

Fig. 2. TG/MS plot of SE derivative: —, TG and DTG curves; -○-, water (*m*/*z* 18); -▽-, carbon dioxide (*m*/*z* 44); -×-, carbon monoxide (*m*/*z* 28); -□-, methyl ion (*m*/*z* 15); -△-, methane (*m*/*z* 16); -◆-, formyl ion (*m*/*z* 29).

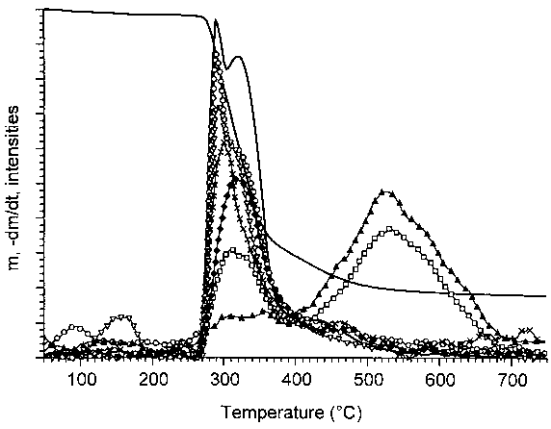

Fig. 3. TG/MS plot of SEA derivative: —, TG and DTG curves; -○-, water (*m*/*z* 18); -▽-, carbon dioxide (*m*/*z* 44); -×-, carbon monoxide (*m*/*z* 28); -□-, methyl ion (*m*/*z* 15); -△-, methane (*m*/*z* 16); -◆-, formyl ion (*m*/*z* 29).

significant. Carbon monoxide (*m*/*z* 28) is produced at about the same level as methane (*m*/*z* 16). There is more CO formed from S, SE, and SEA than methane, while the opposite is true for the rest of the three samples. The fifth most abundant ion is methyl (*m*/*z* 15), while the intensity of other ions decreases as follows: formyl (*m*/*z* 29), formaldehyde (*m*/*z* 30), acetyl (*m*/*z* 43), methoxyl (*m*/*z* 31), acetone (*m*/*z* 58), *m*/*z* 84, and furaldehyde ions (*m*/*z* 95 and 96). The ion *m*/*z* 84 might be 2-methylcyclobutanone or γ-crotonolactone as tentatively assigned before (Kaaden, van der Haverkamp, Boon & de Leeuw, 1983), but according to us also 1,4-dioxadiene.

The TG/MS plot of SE derivative is shown in Fig. 2. This sample has the DTG curve maximum at higher temperature than S due to cross-linking with E. It results in decreased amount of water formed due to dehydration, which is the predominant degradation reaction, but the amount of water is the smallest from all the samples studied (Table 1). The CO_2 ion has a shoulder coinciding with all the less intense ions. It has similar total intensity as CO, which has its maximal formation rate at slightly higher temperature than CO_2. The fourth most intense ion is formyl (*m*/*z* 29), which has its maximum shifted to about 50 K higher temperature, than observed on S, which might be released from C-6 of primary hydroxyls of S after the splitting of the hydroxypropyl etheric linkage. It should be noted that *m*/*z* 29 represents a typical fragment ion of aldehydes (mostly HCHO is evolved), however, some alkane products may form *m*/*z* 29 ion, too. Because the intensities of *m*/*z* 29 and 30 ions are much smaller than that of water and their maxima shifted to higher temperatures, we assume that they could not be considered as primary reaction products. The $-CH_2OH$ group chemistry is different than on lignin, where formaldehyde is formed due to the homolytic splitting of C–C bond, which is favored due to presence of aromatic ring (Jakab et al., 1995). Formation of acetaldehyde or acetone from the cross-links is the result of recombination reactions after primary homolytic splitting of etheric bond and/or withdrawal of hydrogen from hydroxypropyl hydroxyl. The methyl and methane are the next most intense ions that are evolved during the charring process from various molecular segments above 400°C. The methyl intensity curve has a first maximum at 374°C that was not observed from S and indicates its origin from hydroxypropyl bridges. This methyl fragment ion may have split off from aldehydes, acetone or aliphatic molecules.

The decomposition of SEA sample is showed in Fig. 3. The DTG curve has two peaks with a first maximum at 288°C and a second one at 320°C. Although could not be exactly compared due to different geometry of the thermobalances used, SEA seems to be thermally more stable than corn starch amylose modified with CHMAC and analyzed at the same heating rate (Aggarwal et al., 1997). Dehydration, CO_2, and CO formation are involved predominantly in the first maximum, while other ions are rather related to the second DTG peak. Methane and methyl as the next most intense ions also have a low-temperature peak close to the second DTG peak, but their intensity maximum is at 528 and 533°C (Table 1). The thermolysis of the three samples discussed above is different as was demonstrated previously by Py–GC/MS (Šimkovic et al., 1997). By introduction of NH_4OH, more hydroxypropylamine side-chains are present in SEA, which are not cross-linking S as it is in SE sample, which results in more secondary reaction products. The formyl ion, as the sixth most abundant ion has its maximum at about the same temperature as the second DTG peak similarly to other products (e.g. acetone and formaldehyde) evolving from the hydroxypropyl segments (Table 1).

On TG/MS, plot of SEA–HCl Sample (Fig. 4) the *m*/*z* 18 ion is the same as the DTG curve, both peaking at 260°C, while the *m*/*z* 44 ion has its maximum at similar temperature (264°C). The maximal intensity of water ion is at lower temperature than for all other samples studied, which indicates that the presence of HCl affects the dehydration more than observed on S, SE, and SEA, although the total amount of water is slightly lower than that from SEA–H_2SO_4 and

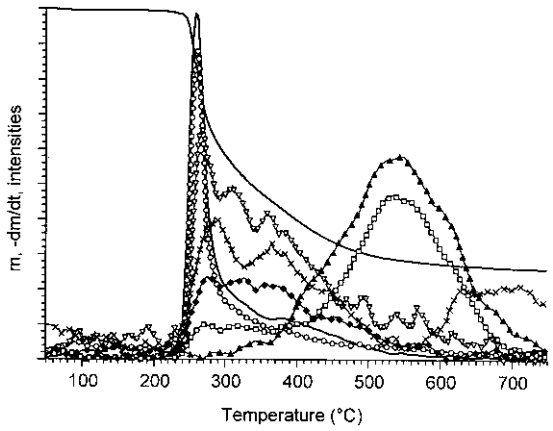

Fig. 4. TG/MS plot of SEA–HCl derivative: —, TG and DTG curves; -○-, water (*m*/*z* 18); -▽-, carbon dioxide (*m*/*z* 44); - × -, carbon monoxide; -□-, methyl ion (*m*/*z* 15); -△-, methane (*m*/*z* 16); -◆-, formyl ion (*m*/*z* 29).

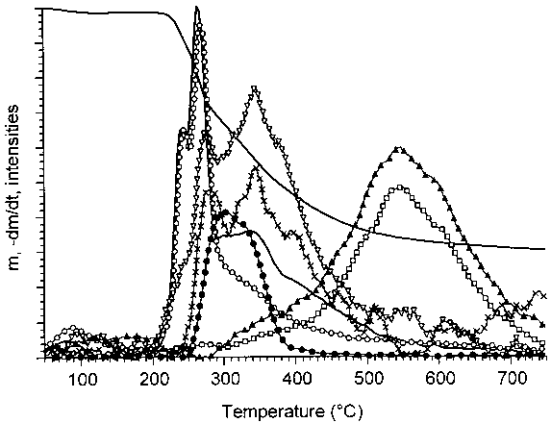

Fig. 5. TG/MS plot of SEA–H_2SO_4 derivative: —, TG and DTG curves; -○-, water (*m*/*z* 18); -▽-, carbon dioxide (*m*/*z* 44); - × -, carbon monoxide (*m*/*z* 28); -□-, methyl ion (*m*/*z* 15); -△-, methane (*m*/*z* 16); -●-, sulfur dioxide (*m*/*z* 64).

SEA–H_3PO_4. The char residue at 750°C is smaller than for the two other acid-treated samples, which indicates that this cycle promotes gasification. There might be also volatile HCl formed, as observed before (Kaaden et al., 1983), however, its main ions (*m*/*z* 36 and 38) can not be detected in the high background of these ions originating from the argon carrier gas. The methoxyl ion has maximum at 225°C (Table 1), which might be also related to the fragmentation of hydroxypropyl bridges, although its intensity is not significant. The methane and methyl ions are the third and fourth most intense ions and CO is the fifth.

SEA–H_2SO_4 sample starts to decompose at the lowest temperature (about 200°C) with a double DTG maximum (Fig. 5). The water ion copies the two maxima of DTG profile (235 and 265°C), indicating that dehydration is the primary reaction. The third decomposition step starts with the evolution of SO_2 (*m*/*z* 64) with maximum at around 305°C, which can be attributed to the decomposition of sulfate groups. Carbon dioxide has its maxima at 278 and 345°C. The broad peaks of CO_2 and CO can be explained by secondary reactions. Less acetone and aldehydes are evolved from the hydroxypropyl units than from the previous samples. On the other hand, SEA–H_2SO_4 releases the highest yield of water and methane so dehydration and methane formation from the hydroxypropyl segments are promoted.

In Fig. 6, the TG/MS plot of SEA–H_3PO_4 is shown. The DTG peak has a main maximum at 278°C and a smaller one at 322°C. The dehydration is very intense similarly to the previous sample (SEA–H_2SO_4) as far as the total amount/yield of water concerned (Tables 1 and 2). However, its decomposition commences at higher temperature with a very high rate and produces a sharp decomposition peak. This sample evolves the lowest yield of methoxyl ion, aldehydes and higher molecular weight products. SEA–H_3PO_4 produces the highest char yield, which might be related to incorporation of phosphorus into the char residue. The second maximum is also related to dehydration, CO and CO_2 formation. Cross-linking of the primary dehydration products with phosphate bridges may occur in the first place while the secondary dehydration results in more condensed residue formed from nitrogen, phosphorus and carbon. The fourth most abundant ion is methane due to free radical recombination at higher temperatures.

3.2. Rates of residue formation and gasification

Most of the proposed mechanisms are based on possibilities and circumstantial evidence instead of unequivocal proof (Shafizadeh, 1968). That is why instead of showing the structural drawings of possible reaction mechanisms giving the prominent volatile products identified, we would prefer to establish only a general equation of thermolysis, which could be covered by thermobalance analysis:

POLYSACCHARIDE → GASES + RESIDUE,

where all the sum of volatiles are considered as gases and the rest, which remains on the themobalance pan is

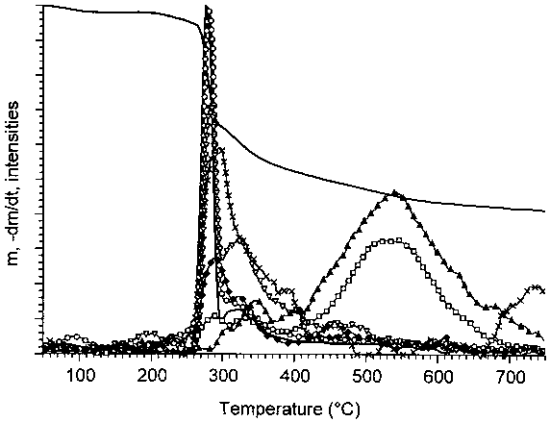

Fig. 6. TG/MS plot of SEA–H_3PO_4: —, TG and DTG curves; -○-, water (*m*/*z* 18); -▽-, carbon dioxide (*m*/*z* 44); - × -, carbon monoxide (*m*/*z* 28); -□-, methyl ion (*m*/*z* 15); -△-, methane (*m*/*z* 16); -◆-, formyl ion (*m*/*z* 29).

Table 3
Results of isothermal TG measurements of starch and its derivatives

Sample	Temperature (°C)						Activation energies (kJ/mol)
	Rate constants[a]						
S		252	263	273	282	292	
	k_r	1.786	4.263	8.572	31.089	67.017	210
	k_g	1.678	1.943	3.954	11.459	12.774	133
SE		252	262	272	282	292	
	k_r	0.092	0.276	0.579	1.473	4.527	206
	k_g	0.081	0.236	0.441	1.039	3.229	218
SEA		242	251	262	272	282	
	k_r	1.331	2.062	4.798	37.189	42.139	231
	k_g	1.292	1.579	4.311	7.123	8.319	124
SEA–HCl		220	231	241	251	262	
	k_r	4.897	12.049	32.206	63.364	237.836	199
	k_g	4.177	8.430	9.906	12.919	19.702	75
SEA–H_2SO_4		220	231	241	251	262	
	k_r	10.858	15.062	17.640	32.614	40.536	72
	k_g	5.783	8.294	10.479	13.901	18.438	60
SEA–H_3PO_4		220	231	241	251	262	
	k_r	1.165	2.985	20.689	26.649	67.709	218
	k_g	0.769	2.302	3.188	9.067	9.190	145

[a] For residue formation, $k_r \times 1000$ (min^{-1}); for gasification, k_g (min^{-1}).

considered as a residue. From the isothermal TG curves, first-order rate constants were calculated as $\ln(m_0/m_t) = f(t)$ by the linear regression method used previously on many models, polysaccharides, and lignocellulose materials (Šimkovic & Csomorová, 1998; Šimkovic et al., 1985a, 1986, 1987a; Šimkovic, Antal & Csomorová, 1989; Šimkovic, Pastúr, Csomorová, Balog & Micko, 1990). They could be considered as the rate constants of residue formation, while the difference between m_0 and m_t is related to the rate of gasification $\{\ln(l/m_0 - m_t) = f(t)\}$ and has not been calculated by this method yet. As seen in Table 3, the rate constants of residue formation are about 1000 times smaller than the rates of gasification. In most cases, the activation energy of residue formation is bigger than for gasification. The rate constants of SE thermolysis are smaller than that of S, while the residue formation activation energy of SE is about the same as for S. The activation energy value for gasification is the highest on SE in comparison to all other samples studied. For SEA, the k_r values increased as well as the corresponding activation energy (E), while the k_g and E values are about the same as for S. The introduction of inorganic acids results in increase of rate constants and decrease of E values as seen for SEA–HCl and especially for SEA–H_2SO_4. The low values for the last mentioned sample might be due to the fact that in this case the corresponding acid was gasified as seen from SO_2 formation. The SEA–H_3PO_4 sample is more stable than SEA–H_2SO_4 and SEA–HCl, which might be due to incorporation of phosphorus into the solid residue leading to formation of P–N bonds in the char. So we can list the decrease of k_r values for individual samples in the order: SEA–HCl > SEA–H_2SO_4 > SEA–H_3PO_4 > SEA > S > SE, while according to their E values the order is: SEA > SEA–H_3PO_4 > S > SE > SEA – HCl > SEA–H_2SO_4. For the gasification, the k_g's are decreasing in the order: SEA–H_2SO_4 > SEA–HCl > SEA–H_3SO_4 > SEA = S > SE while the E's have the following order: SE > SEA–H_3PO_4 > S > SEA > SEA–HCl > SEA–H_2SO_4. This means that the introduction of the weakly basic amine group into the starch polysaccharide (SEA) improves its thermal stability while the bonding of inorganic acids dramatically speeds up the thermolysis of the material.

The instrument was calibrated for water using the dehydration of calcium oxalate monohydrate. Thus, the percentage of water released from the samples during decomposition was calculated and listed in Table 2. About half of the volatile products is water from the original starch sample. The ratio of water/total volatiles decreased significantly for SE and SEA samples due to the high yield of other volatile products from the hydroxypropyl groups. The presence of inorganic acids enhanced the char and water formation and much less other volatiles are observed. The water yield is much more than calculated from amylose samples treated with different inorganic additives, where the sea salt was the most effective with 19.2% of water formed (Kaaden et al., 1983). According to another source (Tomasik et al., 1989), the production of CO_2 and CO up to 1000°C from potato starch was 22 and 34%, respectively, against 32% of other volatiles than water produced from S up to 750°C under different conditions. Also on modified almond shells the dehydration is the predominant reaction as determined by TG/MS run by other research group (Conesa et al., 1997).

4. Conclusions

According to TG/MS results on weakly basic starch-based ion exchanger, the introduction of HCl, H_2SO_4 or H_3PO_4 into the material speeds up the residue formation and gasification reactions of modified polysaccharides, as evaluated by first-order rate constants and activation energies. This is predominantly due to dehydration, which is the most important primary reaction observed, as the majority of other products of thermolysis are formed by secondary or consecutive reactions.

Acknowledgements

This work was supported by the grants 2/6037/99 and 2/7143/20 of the Scientific Grant Agency of Slovak Academy of Sciences (VEGA) as well as by the Hungarian National Research Fund (OTKA No. T025341).

References

Aggarwal, P., Dollimore, D., & Kim, Y. W. (1997). *S.T.P. Pharma Science*, *7* (3), 295–299.

Antal, M., Ebringerová, A., & Micko, M. M. (1991). *Das Papier*, *45*, 232–235.

Antal Jr, M. J., Várhegyi, G., & Jakab, E. (1998). *Industrial Engineering and Chemical Research*, *37*, 1267–1275.

Conesa, J. A., Marcilla, A., & Caballero, J. A. (1997). *Journal of Analytical and Applied Pyrolysis*, *43*, 59–69.

Greenwood, C. T. (1967). *Advances in Carbohydrate Chemistry*, *22*, 483–515.

Jakab, E., Faix, O., Till, F., & Székely, T. (1993). *Journal of Analytical and Applied Pyrolysis*, *25*, 185–194.

Jakab, E., Faix, O., Till, F., & Székely, T. (1995). *Journal of Analytical and Applied Pyrolysis*, *35*, 167–179.

Kaaden, A., van der Haverkamp, J., Boon, J. J., & de Leeuw, J. W. (1983). *Journal of Analytical and Applied Pyrolysis*, *5*, 199–220.

Shafizadeh, F. (1968). *Advances in Carbohydrate Chemistry*, *23*, 419–474.

Šimkovic, I. (1996). *Carbohydrate Polymers*, *31*, 47–51.

Šimkovic, I. (1997). *Carbohydrate Polymers*, *34*, 21–23.

Šimkovic, I., & Csomorová, K. (1998). *Fire Materials*, *22*, 149–154.

Šimkovic, I., Antal, M., Mihálov, V., Königstein, J., & Micko, M. M. (1985a). *Journal of Applied Polymer Science*, *30*, 4707–4711.

Šimkovic, I., Antal, M., Balog, K., Košík, Š., & Placek, J. (1985b). *Journal of Applied Polymer Science*, *30*, 4713–4721.

Šimkovic, I., Ďurindová, M., Mihálov, V., Königstein, J., & Ambrovič, P. (1986). *Journal of Appled Polymer Science*, *31*, 2433–2441.

Šimkovic, I., Hirsch, J., Ebringerová, A., & Königstein, J. (1987a). *Journal of Applied Polymer Science*, *33*, 1473–1477.

Šimkovic, I., Pastýr, J., Antal, M., Balog, K., Košik, Š., & Plaček, J. (1987b). *Journal of Applied Polymer Science*, *34*, 1057–1061.

Šimkovic, I., Varhegyi, G., Antal Jr, M. J., Ebringerová, A., Székely, T., & Szabo, P. (1988). *Journal of Applied Polymer Science*, *36*, 721–728.

Šimkovic, I., Antal, M., & Csomorová, K. (1989). *Journal of Applied Polymer Science*, *38*, 1913–1917.

Šimkovic, I., Pastýr, J., Csomorová, K., Balog, K., & Micko, M. M. (1990). *Journal of Applied Polymer Science*, *41*, 1333–1337.

Šimkovic, I., Balog, K., & Csomorová, K. (1995). *Holzforschung*, *49*, 512–516.

Šimkovic, I., Laszlo, J. A., & Thompson, A. R. (1996). *Carbohydrate Polymers*, *30*, 25–30.

Šimkovic, I., Francis, B. A., & Reeves, J. B. (1997). *Journal of Analytical and Applied Pyrolysis*, *43*, 145–155.

Tomasik, P., Wiejak, S., & Palasinski, M. (1989). *Advances in Carbohydrate Chemistry and Biochemistry*, *47*, 279–344.

Várhegyi, G., Antal Jr, M. J., Székely, T., & Szabo, P. (1989). *Energy and Fuels*, *3*, 329–335.